

Direct evidence of metallicity at ZnO (000 $\bar{1}$)-(1 \times 1) surfaces from angle-resolved photoemission spectroscopy

L. F. J. Piper,^{1,*} A. R. H. Preston,¹ A. Fedorov,² S. W. Cho,¹ A. DeMasi,¹ and K. E. Smith¹

¹*Department of Physics, Boston University, 590 Commonwealth Avenue, Boston, Massachusetts 02215, USA*

²*Advanced Light Source, Lawrence Berkeley National Laboratory, Berkeley, California 94720, USA*

(Received 6 May 2010; revised manuscript received 8 June 2010; published 22 June 2010)

We have investigated the stability of O-polar ZnO (000 $\bar{1}$)-(1 \times 1) surfaces with photoemission spectroscopy and low-energy electron diffraction. We present direct evidence of quasi-two-dimensional electron gas (2DEG) formation ($N_{2D} \leq 2 \times 10^{13} \text{ cm}^{-2}$) at the O-face from our angle-resolved photoemission spectroscopy studies. These findings are discussed in terms of hydrogenation of the O-face by chemisorptions process and the energetic location of the charge-neutrality level of ZnO. Our results reveal insight into the role of hydrogen in forming the quasi-2DEG and stabilizing the O-polar nonreconstructed surface.

DOI: [10.1103/PhysRevB.81.233305](https://doi.org/10.1103/PhysRevB.81.233305)

PACS number(s): 79.60.Bm, 73.20.At

Wurtzite *c*-plane (0001) zinc oxide (ZnO), consists of alternating layers of oppositely charged ions (i.e., O²⁻ and Zn²⁺) stacked parallel to the surface normal resulting in a nonzero dipole moment perpendicular to the surface on all repeat units throughout the material. The termination of the polar ZnO crystal is classified as a Tasker type 3 surface.^{1,2} According to classical electrostatics, ideal bulk-terminated surfaces are unstable a divergent surface energy due to macroscopic electrostatic field. They must be stabilized by the rearrangement of the charge on the outermost layers. The observed stability of both Zn-polar (0001)- and O-polar (000 $\bar{1}$)-(1 \times 1) surfaces presents an intriguing problem to modern surface physics.

Ab initio total energy calculations have suggested that the polar surfaces are stabilized by the removal of the dipole field by an electronic mechanism involving the transfer of 0.17 electrons between them. These calculations also predicted both surfaces are metallic but their metallic nature arises differently.³ This work has promoted various studies of Zn-, O-, and mixed-polar surfaces.⁴ Density-functional theory (DFT) and scanning tunneling microscopy (STM) studies have now concluded that nanosized triangular pits with O-face step edges (effectively O defects) instead facilitate the reduced surface charge on the Zn-polar surface compatible with the charge-transfer model.⁵ However, the corresponding STM of clean O-polar (1 \times 1) surfaces revealed smoother surfaces than for the Zn-polar, with no evidence of nanostructures.⁶ For the O-polar surface hydrogen was instead found to play a significant role in the stabilization of the nonreconstructed surfaces from low-energy electron diffraction (LEED), helium-scattering and x-ray photoemission spectroscopy (XPS) studies by Kunat *et al.*⁷ Interestingly, in the absence of hydrogen a (1 \times 3) reconstruction was observed and a (1 \times 1) pattern was only observed in the presence of small amounts of hydrogen. Electron energy loss spectroscopy (EELS) studies have shown that exposure to hydrogen can result in formation of an electron accumulation space-charge layer near the surface of ZnO, which was removed following either the exposure of oxygen or removal of hydrogen.⁸ A similar result has since been observed with mixed polar (10 $\bar{1}$ 0) ZnO surfaces.⁹ Recent XPS studies have

shown that hydrogen-free O-face surfaces display an absence of downward band bending expected from an electron accumulation profile.¹⁰ Meanwhile, subsequent VB-XPS measurements indicated downward band bending does exist on both polarities and mixed polar surfaces, supported by multiple-field Hall measurements.¹¹

Key to understanding the stability of O-polar surface is elucidating the exact role of the hydrogen. In this Brief Report, we employ a combination of angle-resolved photoemission spectroscopy (ARPES), LEED, and XPS to investigate the electronic and chemical properties of the O-polar (1 \times 1) surfaces. A direct comparison between the O 1s core-level XPS of our (1 \times 1) prepared Zn- and O-polar surfaces indicate that a small amount of hydrogen is present at the O-face. We present direct evidence of quasi-2D electron gas (2DEG) formation ($N_{2D} \leq 2 \times 10^{13} \text{ cm}^{-2}$) from the k_{\parallel} dispersion of the electron sub-band within the electron accumulation layer formed at the hydrogenated O face. These findings are discussed in terms of hydrogenation of the O face by chemisorption and the energetic location of the charge-neutrality level (CNL) of ZnO. Our results reveal insight into the role of hydrogen in forming the 2DEG and stabilizing the O-polar nonreconstructed surface.

Core-level and valence-band XPS measurements were performed at the soft x-ray undulator beamline X1B at the National Synchrotron Light Source (NSLS), Brookhaven National Laboratory, which is equipped with a spherical grating monochromator. Core level XPS spectra ($h\nu=750 \text{ eV}$) were recorded using a Scienta 100 mm hemispherical electron analyzer, with a 0.4 eV total energy resolution for the O 1s region. Binding energies are referenced relative to the binding energy of the Au 4f_{7/2} core level set at 84.0 eV, as measured from a gold foil in electrical contact with the sample. The total instrumental resolution of the VB-XPS, determined from the gold Fermi edge, was approximately 0.35 eV for $h\nu=250 \text{ eV}$. Measurements at X1B were performed at room temperature with a base pressure of 1×10^{-10} torr in the spectrometer chamber. The ARPES experiments were undertaken on undulator beamline 12.0.1 at the Advanced Light Source (ALS), Lawrence Berkeley National Laboratory. This beamline is equipped with a 100 mm hemispherical electron energy analyzer (Scienta SES100). Typical electron energy

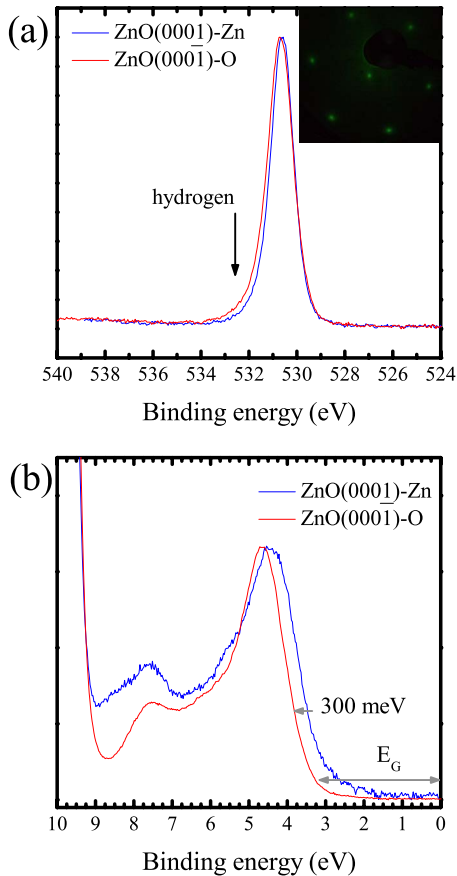


FIG. 1. (Color online) XPS of the (a) O 1s and (b) valence band regions for both ZnO(0001)-Zn or ZnO-(000 $\bar{1}$)-O surfaces following *in-situ* preparation. The inset in (a) displays a typical LEED pattern from the (000 $\bar{1}$)-O surface, with an incident electron energy of 91 eV.

and full angular resolution were 35 meV and 0.5°, respectively. Measurements at BL12.0.1 were recorded at 77 K with base pressure of 4×10^{-11} torr or better in the spectrometer chamber.

The Zn- and O-polar ZnO single-crystals were from Tokyo Denpa Co., LTD., with nondegenerate bulk carrier concentrations of $n = 1 \times 10^{-14}$ cm $^{-3}$. The polar surface orientation [i.e., ZnO(0001)-Zn or ZnO-(000 $\bar{1}$)-O] was confirmed by atomic force microscopy, which revealed triangular pits for the Zn-polar surface only consistent with previous reports.^{5,6} Clean surfaces were prepared in separate ultrahigh vacuum (UHV) preparation chambers directly connected to the spectrometer chambers both at X1B and BL12, with base pressures better than 1×10^{-9} torr. Atomically clean surfaces with sharp (1×1) LEED patterns - as shown in the inset of Fig. 1(a)-were observed for both polarities after cycles of 500 V Ar ion sputtering (1×10^{-5} torr for 20 min) and annealing to 900 K in, followed by annealing in oxygen (1×10^{-6} torr, $T \sim 800$ K, 15 min) and a final flash in UHV (900 K, 5 min). Our recipe for obtaining a (1×1) surface is similar to those reported by Kunat *et al.*,⁷ and Lindsay *et al.*¹² All spectra reported here from surfaces displaying sharp (1×1) LEED patterns. No (1×3) surface reconstructions were observed in our study.

Figure 1(a) displays the O 1s of both faces following surface preparation and confirmation of (1×1) LEED patterns. The increased spectral weight at higher binding energies for the O surface compared to the Zn surface in Fig. 1(a) is consistent with the premise that hydrogen is present on the (1×1) O-polar surface, albeit most likely less than the 1/4 ML expected solely from electrostatic considerations. The O surface is expected to accumulate hydrogen. For instance, Kunat *et al.* concluded that a (1×1) reconstruction was only observed in the presence of hydrogen otherwise a (1×3) reconstruction was seen.⁷ Although this has been disputed by Lindsay *et al.* However, their own HREELS results indicated that 0.05 ML of hydrogen still existed on clean (000 $\bar{1}$)-O surface.¹² The origin of the hydrogen is likely from either dissociated water within the vacuum chamber, or hydrogen from the growth process which has not been completely removed during the annealing process. Further insight has come this year from electrochemical studies, which reported clear differences in the interaction of protons (H^+) and hydroxyls (OH^-) with the two polar surfaces of ZnO.¹³ Using a protic ionic liquid (as the gate dielectric) for ZnO transistors Yuan *et al.*, selectively drove the H^+ or OH^- groups onto ZnO channel surfaces with an electric field. Strong hydrogenation (hydroxylation) via a chemisorption process was observed for O-polar (Zn-polar) surface. For the O-polar surface they concluded that the cycle-dependent enhancement of the surface sheet conductivity (i.e., electron accumulation) was due to an adsorbate (H^+) rather than an electrostatic mechanism. The strong O-H bond in (ZnO-O)-H chemisorption (bonding energy 4.77 eV) from these studies revealed that a large desorption activation energy was required to remove the hydrogen. This finding would support the work of Kunat *et al.*, where a hydrogen-free (1×3) surfaces was only found after many cleaning cycles (up to 50)⁷ and consistent with the premise of residual chemisorbed hydrogen on our (1×1) O-face surfaces.

Figure 1(b) displays the corresponding VB-XPS of both polar surfaces, and reveals that the Fermi levels of both surfaces are pinned close to the CBM of ZnO at room temperature. Our finding would suggest downward band bending and electron accumulation at both surfaces, consistent with reports elsewhere.¹¹ However, we report an increased downward band bending for the O-polar case with a sharp (1×1) LEED pattern. In contrast, Lahiri *et al.* reported that the Fermi level at the Zn surface was pinned close to the conduction band minimum (CBM), while the O surface Fermi level was at the midgap (i.e., 1.2 eV lower in energy) at 600 °C.¹⁰ At these elevated temperatures the O-polar surfaces were free of hydrogen but would rapidly accumulate hydrogen at lower temperatures. Unfortunately no LEED was presented to conclude if the (1×1) O-polar surface could exist H-free in these conditions.

To confirm the presence of H-induced 2DEG formation at the (1×1) O-polar surface we preformed ARPES. Figure 2(a) displays the normal emission ARPES of the H-terminated (000 $\bar{1}$) O-face surface, corresponding to the $\Gamma \rightarrow A \rightarrow \Gamma$ direction in k -space. As in Fig. 1(b), the VBM states appear below 3 eV. However, on closer inspection we observe features within 0.5 eV of the Fermi level at photon

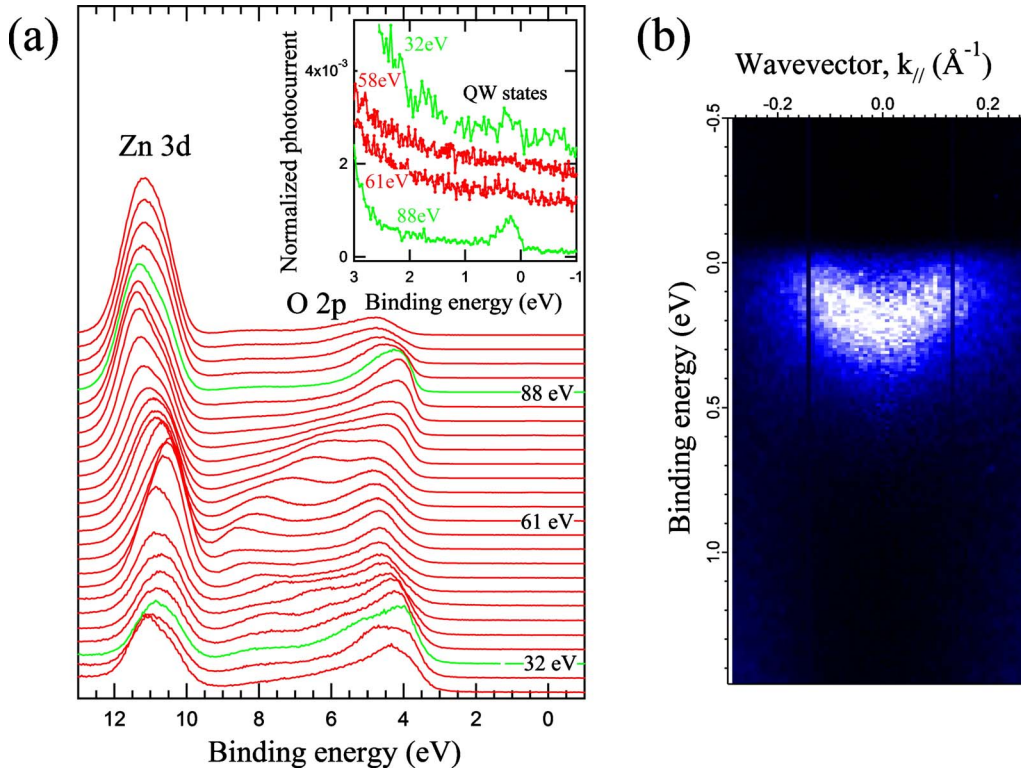


FIG. 2. (Color online) (a) Normal emission ARPES spectra from the $(000\bar{1})$ -O surface, displaying the variation of the semi-core Zn $3d$ and O $2p$ derived valence band region. The inset displays the spectral weight at the Fermi level. Weak features at the Fermi level are observed for 32 and 88 eV, which corresponds to the Γ -point in the k_{\perp} direction. (b) ARPES photocurrent intensity map of the near-Fermi level emission for $h\nu=90$ eV along the $\bar{\Gamma}\rightarrow\bar{K}$ direction in k_{\parallel} -space, recorded at 77 K.

energies of ~ 30 eV and ~ 90 eV. From inspection of the photon-energy dependence and the direct band gap nature of ZnO, we assign these regions as corresponding to the Γ -points. The weak spectral features are then associated with quantized electron sub-band states within the potential well formed by the band bending. The weaker subband intensity at 30 eV is likely associated with the mixed O $2p$ -Zn $4s$ character of the sub-band state. Comparing the O $2p$ and Zn $4s$ cross-sections, we note that $4s$ cross section is greatest around 100 eV (~ 0.1 Mbarn) and rapidly decreases for lower energies (i.e., $< 1 \times 10^{-4}$).¹⁴ In contrast the O $2p$ cross-section continues to increase with reducing photon energy reaching 10 Mbarn at the lowest energies.¹⁴ The dispersion of these states along the $\bar{\Gamma}\rightarrow\bar{K}$ direction for $h\nu=90$ eV, is shown in Fig. 2(b). From the radius of the sub-band at the Fermi level ($k_F=1.3 \text{ \AA}^{-1}$) one can estimate the sub-band electron density as $N_{2D} \approx 2 \times 10^{13} \text{ cm}^{-2}$. Taken together with the high-temperature VB-XPS of Lahiri *et al.*,¹⁰ we consider the adsorbed hydrogen responsible for the formation of the 2DEG of the O-face (1×1) surface observed in our study at lower temperatures. If we consider each adsorbed hydrogen is contributing one electron, coverage of one hydrogen per 20 unit cell would yield $N_{2D} \approx 2 \times 10^{13} \text{ cm}^{-2}$, which corresponds to the lowest coverage amounts reported by Lindsay *et al.* from HREELS of their $(000\bar{1})$ - (1×1) surfaces.¹²

To further understand the macroscopic origin of the downward band bending in the presence of hydrogen additional experiments were performed in order to determine the

CNL of ZnO. For semiconductors, the distribution of evanescent surface states associated with the breaking of the crystal symmetry at the surface can be characterized by the CNL, which marks the energy at which the character of the evanescent surface states changes from predominantly donorlike (below) to acceptorlike (above).¹⁵ As a result, if charged states exist on the surface then the Fermi level is ultimately pinned near to the CNL at the surface. Therefore, the near-surface space-charge of a semiconductor can be understood in terms of the location of the bulk Fermi level and CNL of the material, as highlighted with InAs.¹⁶ Due to the localized real-space, and hence extended k -space, nature of these surface states, the CNL lies close to the mid-gap energy, averaged across the Brillouin zone, not just in the center of the direct gap.¹⁷ We have previously discussed how the low CBM at the Γ -point of post-transition metal oxides results in a CNL above the CBM.¹⁸ One method of determining the CNL experimentally is to determine the stabilized Fermi level pinning location, which has been demonstrated by monolayer alkali-metal coverage of clean III-V surfaces.¹⁹ By monitoring the evolution of the work function following deposition of K to achieve monolayer coverage of (1×1) O-face surfaces (not shown here), we determined that the Fermi level is $3.45 \text{ eV} \pm 0.1 \text{ eV}$ above the VBM (0.3 eV above the CBM). This value is consistent with 3.4 eV predicted recently by DFT by Schliefe *et al.*²⁰ This finding explains the observed downward band bending on both polar surfaces. In the case of O-polar the adsorbed hydrogen must facilitate the formation of charged donorlike surface states

that are otherwise absent without hydrogen at elevated temperatures. This could explain the observed difference in VB-XPS between the two polar surfaces at elevated temperature reported by Lahiri *et al.*¹⁰

Regarding the stability of the O-polar surface our data provides insight into the role of hydrogen in stabilizing the (1×1) O-face. It is interesting to note that electron accumulation layers are also observed with wurtzite InN surfaces of both polarities,^{21,22} which would suggest a common origin. One possible explanation is the disruption of the macroscopic dipole moment by the strong electric fields associated with the 2DEG formation at the surface. In the case of the (1×1) O-polar surface, adsorbed hydrogen must provide the necessary charged surface states to facilitate the Fermi level pinning near the CNL and 2DEG formation. This could further explain both the lack of downward band bending¹⁰ and (1×3) reconstruction⁷ observed in studies of H-free O-polar surfaces. Meanwhile, the nanosized triangular defects on the Zn-face⁵ may be the microscopic origin of the charged surface states facilitating the 2DEG formation for (1×1) Zn-polar surfaces. This interpretation could also extend to 2DEG formation at interfaces between Tasker types 3 and 1 polar oxide insulators e.g., $\text{LaAlO}_3/\text{SrTiO}_3$.²³

To conclude, we have presented direct evidence of surface metallicity (i.e., quantized electron accumulation) at

$\text{ZnO-(000}\bar{1}\text{)-(1} \times \text{1)}$ surfaces. The (1×1) surface is stabilized by hydrogen adsorbates. The sub-band carrier density was determined to be $N_{2D} \leq 2 \times 10^{13} \text{ cm}^{-2}$ from ARPES. This finding is consistent with our determination that the CNL of ZnO lies near the CBM. This results in the observed downward band bending at the surface in the presence of hydrogen adatoms.

The authors wish to thank M. W. Allen and S. D. Durbin for correspondence regarding the nature of the ZnO films, such as AFM and Hall studies. L.F.J.P. also acknowledges fruitful discussions with S. Senanayake, and F. Bechstedt. The Boston University program is supported in part by the Department of Energy under Contract No. DE-FG02-98ER45680 and by the Donors of the American Chemical Society Petroleum Research Fund. This work was also supported in part by the Department of Energy under Contract No. DE-FG02-98ER45680. The NSLS was supported by the U.S. Department of Energy, Office of Science, Office of Basic Energy Sciences, under Contract No. DE-AC02-98CH10886. The Advanced Light Source is supported by the Director, Office of Science, Office of Basic Energy Sciences of the U.S. Department of Energy under Contract No. DE AC0205CH11231.

*lfj Piper@bu.edu

¹P. W. Tasker, *J. Phys. C: Solid State Phys.* **12**, 4977 (1979).

²C. Noguera, *J. Phys.: Condens. Matter* **12**, R367 (2000).

³A. Wander, F. Schedin, P. Steadman, A. Norris, R. Mc-Grath, T. S. Turner, G. Thornton, and N. M. Harrison, *Phys. Rev. Lett.* **86**, 3811 (2001).

⁴C. Woll, *Prog. Surf. Sci.* **82**, 55 (2007).

⁵O. Dulub, U. Diebold, and G. Kresse, *Phys. Rev. Lett.* **90**, 016102 (2003).

⁶U. Diebold, L. V. Koplitz, and O. Dulub, *Appl. Surf. Sci.* **237**, 336 (2004).

⁷M. Kunat, S. G. Girol, T. Becker, U. Burghaus, and C. Woll, *Phys. Rev. B* **66**, 081402(R) (2002).

⁸A. Many, I. Wagner, A. Rosenthal, J. I. Gersten, and Y. Goldstein, *Phys. Rev. Lett.* **46**, 1648 (1981).

⁹Y. Wang, B. Meyer, X. Yin, M. Kunat, D. Langenberg, F. Traeger, A. Birkner, and C. Woll, *Phys. Rev. Lett.* **95**, 266104 (2005).

¹⁰J. Lahiri, S. Senanayake, and M. Batzill, *Phys. Rev. B* **78**, 155414 (2008).

¹¹M. W. Allen, C. H. Swartz, T. H. Myers, T. D. Veal, C. F. Mc-

Conville, and S. M. Durbin, *Phys. Rev. B* **81**, 075211 (2010).

¹²R. Lindsay, C. A. Muryn, E. Michelangeli, and G. Thornton, *Surf. Sci.* **565**, L283 (2004).

¹³H. Yuan, H. Shimotani, A. Tsukazaki, A. Ohtomo, M. Kawasaki, and Y. Iwasa, *J. Am. Chem. Soc.* **132**, 6672 (2010).

¹⁴J. J. Yeh and I. Lindau, *At. Data Nucl. Data Tables* **32**, 1 (1985).

¹⁵W. Monch, *Semiconductor Surfaces and Interfaces* (Springer, Berlin, 2001).

¹⁶L. F. J. Piper, T. D. Veal, M. J. Lowe, and C. F. Mc-Conville, *Phys. Rev. B* **73**, 195321 (2006).

¹⁷J. Tersoff, *Phys. Rev. Lett.* **52**, 465 (1984).

¹⁸L. F. J. Piper *et al.*, *Phys. Rev. B* **78**, 165127 (2008).

¹⁹M. G. Betti, V. Corradini, G. Bertoni, P. Casarini, C. Mar-iani, and A. Abramo, *Phys. Rev. B* **63**, 155315 (2001).

²⁰A. Schleife, F. Fuchs, C. Rodl, J. Furthmuller, and F. Bechstedt, *Appl. Phys. Lett.* **94**, 012104 (2009).

²¹I. Mahboob, T. D. Veal, C. F. McConville, H. Lu, and W. J. Schaff, *Phys. Rev. Lett.* **92**, 036804 (2004).

²²R. P. Bhatta, B. D. Thoms, M. Alevi, and N. Dietz, *Surf. Sci. Lett.* **601**, L120 (2007).

²³A. Ohtomo and H. Y. Hwang, *Nature (London)* **427**, 423 (2004).